DOI: 10.64302/joshusc.v35n2.1425

ULTRASONIC SYNTHESIS OF STARCH-MATRIX SILVER NANOPARTICLES AND PRELIMINARY TEST OF DOXORUBICIN LOADING CAPABILITY

Tran Ngoc Diem[1], Nguyen Vinh Phu[2], Nguyen Thi Thanh Tuyen[1], Ngo Khoa Quang[3], Bui Quang Thanh*[1]

[1]Faculty of Chemistry, University of Sciences, Hue University

[2]Faculty of Basic Sciences, University of Medicine and Pharmacy, Hue University

[3]Faculty of Electronics, Electrical Engineering, and Material Technology, University of Sciences, Hue University

*Email: thanh.bui@hueuni.edu.vn

Received: 24/3/2026; Received in revised form: 6/5/2026; Accepted: 19/6/2026

ABSTRACT

Silver nanoparticles (AgNPs) exhibit pH-responding affinity for doxorubicin, but challenges remain in their aqueous-mediated stabilisation and synthesis-related toxicity. This study investigated a green synthesis of AgNPs for its optimisation, followed by a preliminary screen for their doxorubicin-loading capability. The optimal procedure includes biocompatible reagents only, i.e.: $AgNO_3$ (precursor), D-glucose (reductant), starch (stabiliser), and aq. NaOH (pH adjuster), coupled with an ultrasonic bathing (42 kHz; 100 W) and room temperature (25 °C). The starch-matrix AgNPs were successfully synthesised and characterised by UV-Vis spectroscopy (λ_a 400 nm; I_a 3.0-3.5 abs., $\overline{D}_{size(UV-Vis)}$ 20-45 nm), XRD (2θ = 38.1° (111), 44.3° (200), 64.4° (220), 77.4° (311); JCPDS 04-0783; $\overline{D}_{size(XRD)}$ ca. 15 nm), SEM (AgNPs-starch morphology; $\overline{D}_{size(SEM)}$ 10-30 nm), EDX (C: 0.285 keV; O: 0.525 keV; Na: 1.044 keV; Ag: ~3 keV), and FT-IR (no evidence of functional changes). The nanoparticles demonstrate their ability for pH-responsive doxorubicin loading and release, confirmed by UV-Vis analysis. The results encourage efforts for more in-depth understanding and further in-practice testing.

Keywords: doxorubicin, green synthesis, pH responsiveness, ultrasonics, silver nanoparticles.

1. INTRODUCTION

Cancer chemotherapy is still serving as an important role in oncology, despite its off-targeting problems [1]. The treatment employs cytotoxic drugs to kill rapidly dividing cancer cells or inhibit their growth, thus theoretically expected to eradicate a broad-to-all spectrum of cancerous types. The inevitable downside is that it also induces systemic toxicity onto healthy cells/tissues due to its non-specific bio-selectivity. To overcome this challenge, future research focusing on targeted therapies is still ongoing; particularly, drug-nanocarrier delivering systems have attracted special attentions from scientific community as promising tools.

Environmental pH is one of the most attractive stimuli for drug delivery systems regarding cancer treatment. In fact, tumour tissues are well-documented to have a more acidic microenvironment (pH ranging from 7 to 6) compared to normal tissues (pH ~7.4) [2]; thus, pH-sensitive drug carriers have gained a raising attention from scientific community. This sensitivity is often exploited from either pH-triggered chemical transformations of functional groups (e.g. hydrazone, imine, ester, or amide bonds) or modulation of weak interactions (e.g. hydrogen bonding, van der Waals forces, dipole interactions, or π-stacking) [3]. However, the former inevitably contains bio-hazardous chemicals meanwhile, the latter apparently raises concerns on the loading capacity.

Doxorubicin (marketed under the brand name Adriamycin) is a broad-spectrum anthracycline-class chemotherapeutic agent, effective to a wide variety of solid tumors and blood cancers. The drug was first-time isolated from *Streptomyces peucetius* in the 1960s [4], approved by U.S. Food and Drug Administration in 1974 and listed in the World Health Organization's List of Essential Medicine recently [5]. The medicine has been profiled for its non-selective cytotoxicity and adverse side effects, including myelosuppression, alopecia, and gastrointestinal disturbances, along with potential hypersensitivity reactions ranging from skin rashes to anaphylaxis [6]. Nevertheless, doxorubicin remains indispensable in cancer treatment owing to its clinical effectiveness at the expense for its manageable toxicity.

Silver nanoparticles (AgNPs) possess special physicochemical properties as a potential delivering agent in design of the drug-nano systems. The noble metal nanoparticles have been known for their strong affinity for functional groups containing S, N, and O (commonly found in drug molecules and biological macromolecules) coupled with their biological compatibility and safety in the body. However, conventional chemical synthesis of AgNPs often involves physio-toxic reductants and surfactants, raising other concerns the potent side effects. Some approaches utilised natural extracts as reducing, capping, and stabilising agents for green syntheses of the inorganic nanoparticles. To this, the promising upside is that this is reasoned for synergistic effects if using pharmaco-valuable plants, herbs, or other microorganisms [7]

and for the biological compatibility; the inherent downside is of the concern regarding mass-production cost and low-controllable quality.

Starch is a biodegradable and cost-effective polysaccharide, which is also able to be obtained from industrial production under analytical controllability. Its hydroxyl-rich structure allows the compound to serve as a potential bio-surfactant for nanoparticle synthesis via metal-ion reduction and colloidal stabilisation, thus potentially improving dispersibility, enhancing biocompatibility, and reducing cytotoxicity of the starch-capped nanocarriers [8]. Also, starch is considered especially suitable for drug-delivery applications given its bioactive interactions with extracellular structures [9]. However, using scaffold-polymeric surfactants (such as starch in this case) for nanomaterial synthesis would often result in particle-size uniformity and overgrowth, likely caused by uniform-steric capsulation and gradual-kinetic reduction [10]. Hence, further technically assisting are necessary in order to either improve the synthesis procedures or increase the nanomaterial products.

Ultrasonics is extensively used in chemical synthesis and colloidal dispersion due to its unique physical effects. While shockwave-assisted techniques had been well-established for macroscale applications (e.g., sonochemistry, cleaning), their nano-specific mechanisms were also proved with a unique physical approach to controlling nanoparticle surface stability during synthesis (e.g., silica coating on magnetite) [11]. When high-frequency ultrasound (20 kHz - 15 MHz) propagates through a liquid medium, the implosive collapse of cavitation bubbles produces localised shockwaves with extreme pressures (ca. 60 kbar) and rapid fluid dynamics (microjets reaching hundreds of $m.s^{-1}$) [12]. These transient mechanical forces are thought to be considered as effective surface protectants and efficient mass transfer of Ag^+ ions to nucleation sites (of the polysaccharide branched matrix).

In this work, an extended approach was carried out to investigate the preparation of biocompatible AgNPs materials and test the pH-responsive ability of doxorubicin-AgNPs nanocarriers. Different reacting conditions for a green synthesis of the nanoparticles were systematically examined in order to find an optimal procedure. The as-obtained nano-system was subjected to a further test for drug-loading capacity and its pH-triggered response.

2. METHODOLOGY

2.1. Preparation of starch-AgNPs

The preparation of starch-capped silver nanoparticles (AgNPs) was systematically studied under four distinct reaction conditions and two approaches for purfication. The standardised synthetic procedure includes three sequential stages: (i)

starch-colloidal stabilisation, (ii) silver-precursor introduction, and (iii) starch-AgNPs formation. Initially, starch solutions (32 mL; 0.2% w./v.) were prepared under controlled conditions (30 ± 2°C; 30 min). Following the stabilisation, $AgNO_3$ aq. solution (16 mL; 0.001 M) was introduced into each of the samples, with gradual heating (to a testing temperature). Finally, the reduction step was initiated by the addition of reductive agents. The reaction mixture was maintained at an unchanged temperature (1 hour) with continuous application of the respective dispersion method (either mechanically or ultrasonically) throughout the synthesis durations. The products were purified using different techniques (either centrifugally or dialytically), before delivered for further characterisation or dried (70 °C) for solid-state storage.

Regarding the surveying conditions, dispersion approach was either magnetic stirring (1500 rpm) or ultrasonic processing (100 W, 42 kHz); the reductive agent was either D-glucose aq. or $NaBH_4$ aq. solution (0.5 mL; 0.1 M); the medium pH was adjusted using either NaOH aq. or NH_3 aq. (2.5 mL; 0.1 M); subsequently, the reacting temperature was controlled at either 25 °C (room temperature), 40 °C, or 60 °C for each main surveying condition. The corresponding experimental settings for condition surveying are summarised in Table 1.

Table 1. Controlled conditions for preparation of AgNPs

	Dispersion		Reductant		pH adjuster		Temperature
	Stirring	Ultrasonics	$NaBH_4$	D-glucose	NH_3	NaOH	25/40/60 °C
Sample 1	(+)		(+)		(+)		(+)
Sample 2	(+)			(+)	(+)		(+)
Sample 3	(+)			(+)		(+)	(+)
Sample 4		(+)		(+)		(+)	(+)

(+): positive

Regarding the purifying techniques, the starch-AgNPs colloidal obtained from the optimal synthesis procedure (i.e. S4(25) in this report) was subjected to either centrifugation (9000 rpm) or cellophane dialysis (5-6 hrs), notated as S4(25) and S5(25) respectively. The corresponding characterision settings for samples obtained from different purification techniques are summarised in Table 2.

Table 2. Purifying techniques for preparation of AgNPs

	Purification	EDX	XRD	SEM	FTIR
Sample 4	Centrifugation	(+)			
Sample 5	Dialysis	(+)	(+)	(+)	(+)

(+): positive

2.2. Loading of doxorubicin

AgNPs obtained under the optimal synthesis condition was used for preparation of doxorubicin carrier. Typically, pharmaceutical-grade doxorubicin hydrochloride (2 mg/mL; 0.2 mL) was introduced to the freshly prepared starch-AgNPs suspension (10 mL). The mixture was constantly dispersed using a laboratory shaker (250 rpm; 24 hrs; room temperature) for loading process. Afterwards, the colloidal was titrated with unbuffered hydrochloric acid solution (pH 1) to achieve refreshed pH values (6.5 and 7.5); the samples were shaken for dispersion (250 rpm; 1 hr; room temperature). Finally, the suspensions were collected and sent for UV-Vis spectroscopic analysis to relatively quantify the drug-loading capacities; the bulk-available components were related to their corresponding peak intensities in the optical spectra.

2.3. Characterisations

All chemicals were used as received without further purification. In particular, pharmaceutical-grade doxorubicin hydrochloride ("Ebewe", 50 mg/25mL) was obtained from EVER Pharma GmbH (Austria); silver nitrate (99.8+%) was delivered from Fisher Scientific (USA); analytical-grade hydrochloric acid (0.1 N standard solution), sodium hydroxide (> 99+%), starch soluble, sodium borohydride, and D-glucose monohydrate were purchased from Xilong Scientific (China); distilled water was used in all steps.

UV-Visible absorption spectra were recorded using a Genesys 10S UV-Vis spectrophotometer (Thermo Scientific, USA) with spectral scanning from 300 to 700 nm. Crystalline structure of the synthesised nanoparticles was analysed using X-ray diffraction (XRD; D8-Bruker, Germany) with Cu Kα radiation (λ = 1.5406 Å); further, the average crystallite size was determined using Scherrer's equation [13]. Functional changes were monitored using Fourier-transform infrared spectroscopy (FT-IR; Shimadzu IR Prestige-21, Japan). Elemental composition was determined using energy-dispersive X-ray spectroscopy (EDX; JEOL JED-2300, Japan). The UV-Vis peaks were deconvoluted using Multiple Peak Fit tool (Origin 2024; OriginLab Corporation).

3. RESULTS AND DISCUSSION

3.1. Starch-AgNPs nanocomposite

The UV-Vis spectra measured from the synthesised nanoparticle colloids by all the experimental settings were presented in Figure 1. According to preceding work, the particle size and distribution of AgNPs can be preliminarily estimated using the UV-Vis optical morphologies [14]; particularly, the former is directly related to the peak position while the latter can be assessed from the peak area. Also, the peak height is well known to be related to the concentration of AgNPs yielded in the colloid. Therefore, the results collected from UV-Vis data can serve as an effective parameter of survey for AgNPs

synthesis across the procedural settings.

Overall, the increase of reaction temperature induces absorption intensity yet peak red-shifting, and vice versa. This means following the rise of synthesis temperature, the productivity tends to increase while the quality appears to be downgraded. The upside patterns are expected as high temperature leads to faster reaction rates via the increase of molecular/particle kinetic energy, causing them to collide more frequently and greater forcefully. On the other hand, the cost is the induction of condensational growth (i.e. Ostwald ripening process), forming heterogeneous and overring-sized nanoparticles as the final products [11]. Thus, effective solutions to exploit the thermal push of precursor molecules while deteriorate the surface activity of nuclear crystallites are still needed.

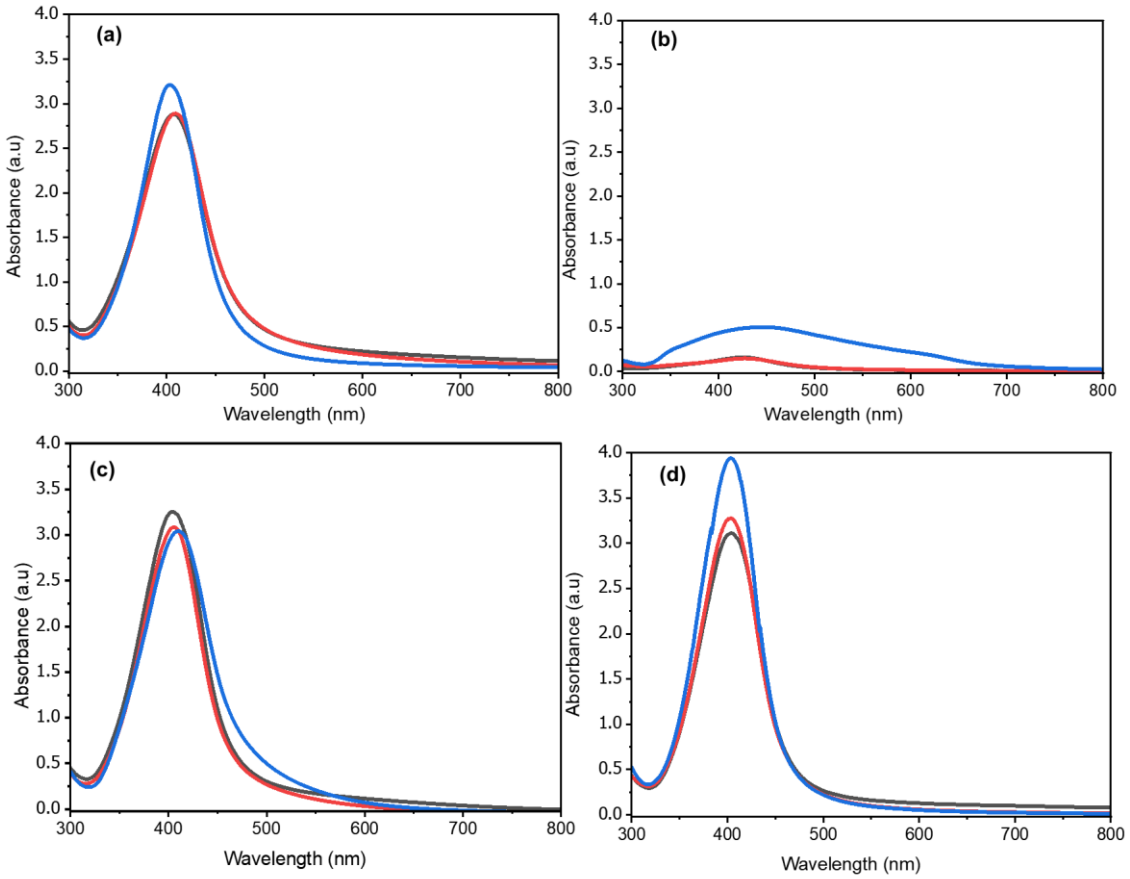


Figure 1. UV-Vis spectra of all synthesised nanoparticle samples: (a) S1; (b) S2; (c) S3; (d) S4; temperature: (black) 25 °C, (red) 40 °C, (blue) 60 °C

First, a conventional procedure (i.e. S1) using $NaBH_4$ (a strong reactant) and NH_3 aq. (a weak base) was carried out with a mechanical dispersion (magnetic stirring); the UV-Vis spectra are presented in Figure 1a. Given all the tested temperatures, the reaction colloid changed its colour to yellow immediately with the introduction of $NaBH_4$ solution and stabilised its opacity under the following 1 minute, indicating the rapid

formation of silver nanoparticles. The optical absorption registers the optimal values (ca. 3.0 abs and 400 nm) at 60 °C, slightly better than those (ca. 2.9 and 405 nm) at the lower temperature, aka. 25 and 40 °C. The observables can be explained the predominant chemical kinetics (contributed by the high reactivity of $NaBH_4$) regardless of the reacting thermal kinetics (from the environmental temperature). However, while NH_3 can be easily removed from the final product by appropriate vaporisation, $NaBH_4$ is well-known and proved for its persistent remaining and severe toxicity. This means looking for more health-friendly (and possibly equivalent reductant capacity) agents is necessary for further bio-chemo-directed applications.

Second, a modified procedure (i.e. S2) using D-glucose (a bio-available compound) as the alternative reductant was proposed; the UV-Vis spectra are presented in Figure 1b. Given the experimental phenomena, S2(25) was almost no change in colour by eye-based observation, yet became very-pale yellow after 24 hr; S2(40) changed to very-pale yellow after 30 min of reaction and remained apparently unchanged after 24 hr; S2(60) turned to pale yellow after 20 min and stabilised as a brownish colloid after 180 min. In their corresponding UV-Vis spectrum, the lower-temperature samples possess almost negligible intensities (ca. 0.1 abs and 425 nm); meanwhile, the higher-temperature counterpart registers a very broaden peak from 350 to 650 nm (ca. 0.5 abs and 450 nm). The observables indicate that not only the settings are not productive but also the products are not homogeneous in size, likely caused by the overall drop of kinetic strength. This suggests further test on stronger bases as the environment.

Hence, aq. NaOH (with only bio-compatible components) was used in the next-step procedure (i.e. S3) for the survey; the UV-Vis spectra are presented in Figure 1c. Given this consideration, all the samples changed their colour immediately after the introduction of D-glucose solution; afterwards, they were darkening gradually and stabilised at 5th minute for S3(25), 4th minute for S3(40), and and 1st minute for S3(60). Analysing their spectrum, the recorded pattern follows the thermal kinetics consistently; in other words, the increase of reaction temperature tends to shift the maximal peaks towards reddish region and broaden the spectral shoulders. The optimal condition is considerable at 25 °C (ca. 3.2 abs and 410 nm); others follow with considerably marginal differences towards lower-intensity and red-shifted tendencies. The deintensification can be explained by the Ostwald-ripening inertia. Regarding the pre-proved evidences for its micro-kinetical and surface-protective advantages, ultrasonics can be utilised to potentially improve the current apparatus.

Finally, ultrasonic bathing was applied as an assistant technique for the potentially improved procedure (i.e. S4); the UV-Vis spectra are given in Figure 1d. From the initiation, the reaction colour was changed almost immediately, then darkening gradually, finally stabilised at brownish yellow since 10th minute for S4(25), 6th minute for S4(40), and 3rd minute for S4(25). Concerning the corresponding data, absorption

intensities were a slight improvement aligned with low-to-high tendency of temperature (ca. 3.0-3.5 abs), the characteristic wavelengths see no noticeable differential (ca. 400 nm). The phenomena suggest that the ultrasonic surface-protective property is likely independent on and probably dominating the thermal Ostwald-ripening potentiality. This means the quality-optimal condition is at room temperature (aka. 25 °C) for convenience, while elevated temperatures are for quantity-related consideration. Also, the consistent positioning of peaks regardless of reaction temperature might imply a low-bound threshold for particle size under our apparatus setting (i.e. 42 kHz - 400 nm); the average value can be estimated to be approx. 45 nm (using Amirjani et al. equation [14]) or ca. 20 nm (using Paramelle et al. model [15]).

The EDX data of starch-AgNPs after being purified using centrifugation (sample S4(25)) and cellophane dialysis (sample S5(25)) are given in Figure 2. In general, there are three main elements detected, including C (0.285 keV), O (0.525 keV), and Ag (ca. 3 keV); characterised for surface plasmon resonance of AgNPs. In particular, using centrifugation was unlikely to be an effective separation of the obtained starch-AgNPs from the precursor residues given by the peak of Na (1.044 keV); meanwhile, it is clear that by utilising dialysis through cellophane membrane, no contaminated traces are probed. The colour-mapping images indicate the even distribution of the primary elements (i.e. C, O and Ag), thus proving both the effective incorporation of AgNPs into starch matrix and the uniform dispersion of the metallic-matrix systems. Regarding all the primary elements, i.e. C (red), O (green), and Ag (cyan), their even colour-mapping confirms their uniform matrix-distribution, demonstrating the successful integration of AgNPs into starch matrix to form a homogeneous composite system.

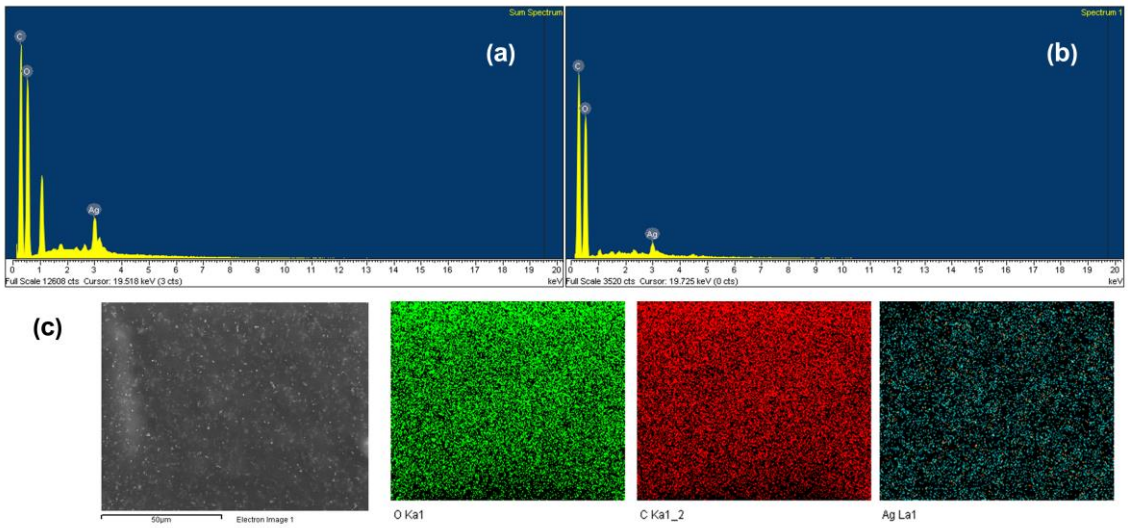


Figure 2. EDX data of starch-AgNPs: (a) purified using centrifugation - S4(25); (b) purified using dialysis - S5(25); (c) element mapping analysis - S5(25)

The XRD pattern measured on the solid samples of S5(25) is plotted in Figure 3. The distinct peaks observed at characteristic 2θ positions of 38.1° (111), 44.3° (200), 64.4° (220), and 77.4° (311) correspond to the face-centred cubic (fcc) crystal structure of metallic silver (Ag; JCPDS 04-0783). Using Scherrer's equation with full-width at half-maximum values for the strongest peak (i.e. 111), the average crystallite size is estimated ca. 15 nm - thus possibly smaller than other measurements. Besides, the starch matrix is related to a high-intense broad peak from 15° to 30° characterised for amorphous phases. The information altogether confirms the structural integrity of the silver nanoparticles particularly, and the successful formation of starch-AgNPs matrix generally.

The SEM images of starch-AgNPs (sample S4(25)) are presented in Figure 4. The electron-scanning images reveal the homogeneous particles sized in nanometer-scales (brighter and discrete dots), attached onto the surface of heterogeneous matrix (darker and gelatinated background). The former indicates the successful synthesis of Ag nanoparticles, whose size is ca. 10-30 nm thus consistent with those calculated from the corresponding UV-Vis spectrum and XRD pattern. The later reveals that gelatination of starch during the experiments, which is thought to be conducive to biological compatibility backed by its highly aqueous solubility. In fact, the obtained colloid can remain its stably homogeneous dispersion with no visible signs of aggregation were observed over the observation period of four weeks.

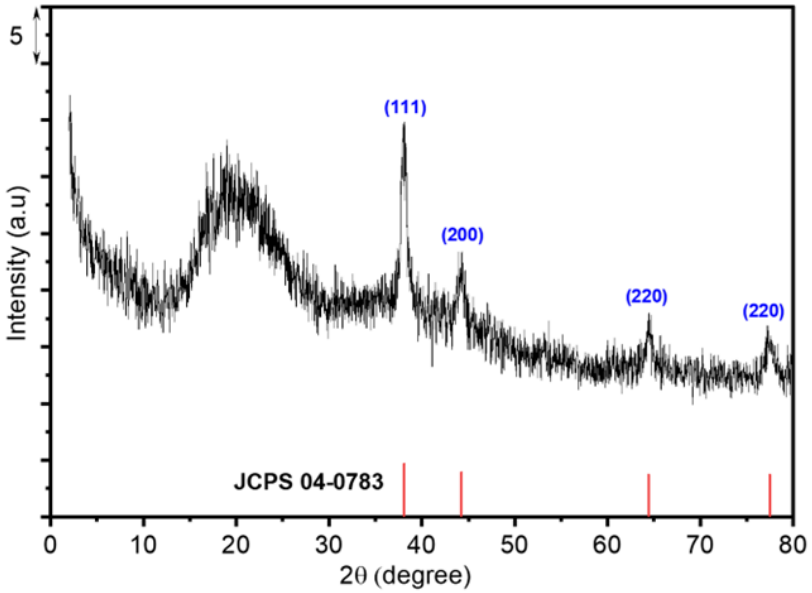


Figure 3. XRD pattern of S4(25) and the standard JCPDS 04-0783

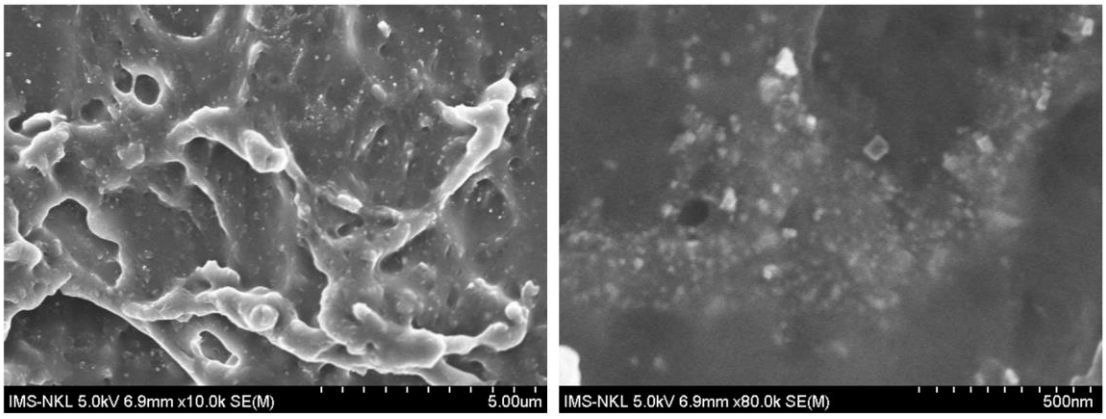


Figure 4. SEM images of S4(25)

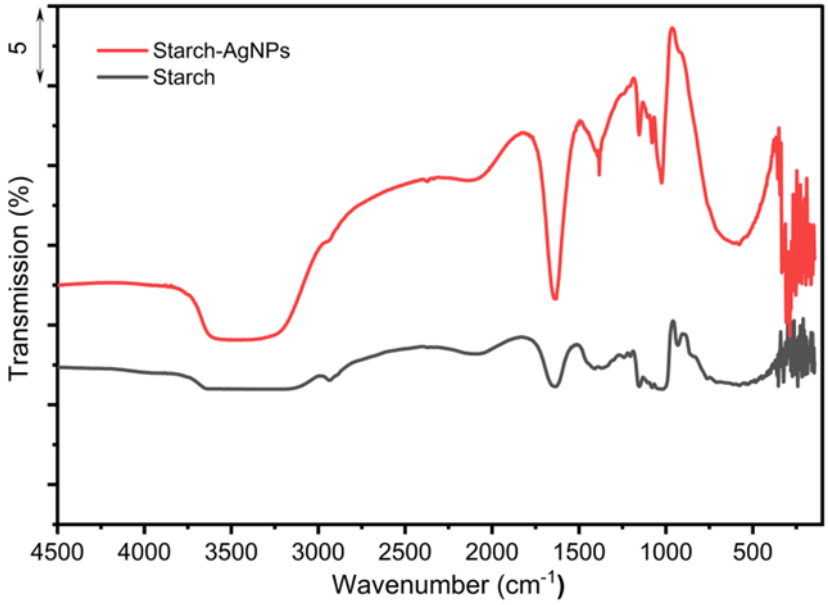


Figure 5. FT-IR spectra of starch-AgNPs and pure starch (as a reference)

The FT-IR spectrum of starch-AgNPs compared to those from a pure-starch sample as the reference for the functional changes (if any) are presented in Figure 5. Given the carbohydrate matrix, the characteristic peaks for starch can be clearly observed, i.e.: broadened 400-900 cm^{-1} (C-O-C ring vibration), 1020.34 to 1103.28 cm^{-1} (C-O stretching), 1153.43 cm^{-1} (C-O-C asymmetric stretching) [16]. In terms of the nanocomposite, the respective peaks are broadened 400-900 cm^{-1}, 1024.20 to 1103.28 cm^{-1}, 1153.43 cm^{-1}. These measurable differences are considered insignificant for any chemical functionalisation, thus implicating that the starch and AgNPs are likely interacting through steric coating rather than covalent bonding.

3.2. Doxorubicin loading and release

The loading of doxorubicin onto the as-prepared nanocarriers was subjected to an experimental test under different pH values. The bulk availability of the drug was measured and compared by UV-Vis spectroscopics in different pH values.

The UV-Vis spectra of doxorubicin-AgNPs suspensions are given in Figure 6. After deconvolution of overlapping peaks, the intensity ratios between AgNPs-characteristic peak and doxorubicin-specified counterpart are profoundly different when comparing the tested pHs. In particular, the ratio is over 3:1 at pH 7.5, while the corresponding value for pH 6.5 is approximately 1:1. The explanation is that the drug is likely to be absorbed onto the nanoparticles in the acidic pH, while be released into the bulk medium in the neutral environment. Also, although the optical absorbance is varied significantly across the pH changes, the overall characteristic wavelengths are almost intact, thus preliminarily suggesting a binding mechanism based on weak field forces (e.g. hydrogen or van der Waals interactions) rather than on strong chemical bonds. The negative control demonstrates that the spectral profile of doxorubicin remains relatively stable across the tested range. This confirms that the pH sensitivity is a direct result of the drug-nanoparticle interaction, rather than a chemical change of the drug.

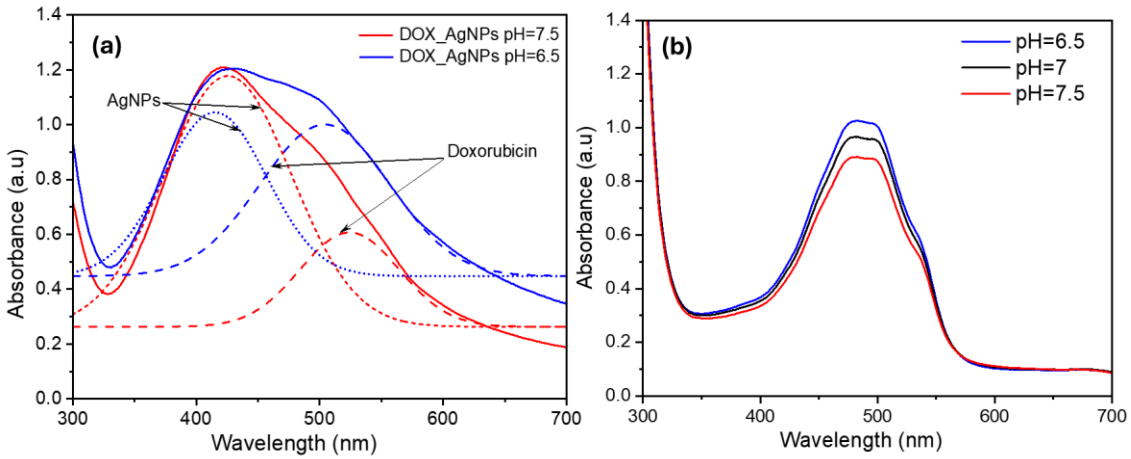


Figure 6. UV-Vis spectra of doxorubicin-AgNPs suspensions: (line) pH 7.5; (dot) pH 6.5

4. CONCLUSION

This work investigates the green synthesis of starch-AgNPs nanocomposite and its capacity to load/release doxorubicin. The optimal procedure utilised the protective properties of ultrasonic bathing (42 kHz; 100 W) at room temperature (25 °C) with the bio-compatible reactants including $AgNO_3$ (precursor), D-glucose (reductant), starch (stabiliser), and aq. NaOH (environment). The starch-coated AgNPs colloid was successfully prepared, confirmed by UV-Vis spectroscopy (wavelength 400 nm; intensity

3.0-3.5 abs; average size ca. 20-45 nm), XRD pattern (2θ: 38.1° (111), 44.3° (200), 64.4° (220), and 77.4° (311); JCPDS 04-0783; average size ca. 15 nm), SEM images (morphology: Ag nanoparticles attached onto gelatinated-starch matrix; average size ca. 10-30 nm), EDX analysis (elements: C (0.285 keV), O (0.525 keV), and Ag (ca. 3 keV)), and FT-IR spectroscopy (no evidences for chemical functionalisation). The capacity for doxorubicin loading/release was proved with respect to pH changes using UV-Vis probing. The results are conducive to further attempts for in-depth investigation (e.g. on more accurate mechanism) and extended applications (e.g. on *in vitro* testing).

ACKNOWLEDGMENTS

The research was financially supported by University of Sciences, Hue University [ĐHKH2026B-023; Tran Ngoc Diem] and partially facilitated by Professor Nguyen Thi Ai Nhung under Hue University - Core Research Programme [NCTB.DHH.2024.04].

REFERENCES

[1]. Behranvand N, Nasri F, Zolfaghari Emameh R, Khani P, Hosseini A, et al. (2022). Chemotherapy: a double-edged sword in cancer treatment. *Cancer Immunol. Immunother.* Vol. 71(3), pp. 507–26.

[2]. Liu J, Huang Y, Kumar A, Tan A, Jin S, et al. (2014). pH-sensitive nano-systems for drug delivery in cancer therapy. *Biotechnol. Adv.* Vol. 32(4), pp. 693–710.

[3]. Ding H, Tan P, Fu S, Tian X, Zhang H, et al. (2022). Preparation and application of pH-responsive drug delivery systems. *J. Control. Release*. Vol. 348(June), pp. 206–38.

[4]. Bonadonna G, Monfardini S, de Lena M, Fossati-Bellani F. (1969). Clinical evaluation of adriamycin, a new antitumour antibiotic. *Br Med J*. Vol. 3(5669), pp. 503–6.

[5]. https://www.who.int/publications/i/item/WHOMVPEMPIAU2019.06

[6]. van der Zanden SY, Qiao X, Neefjes J. (2021). New insights into the activities and toxicities of the old anticancer drug doxorubicin. *FEBS J.* Vol. 288(21), pp. 6095–6111.

[7]. Nguyen VP, Le Trung H, Nguyen TH, Hoang D, Tran TH. (2021). Synthesis of biogenic silver nanoparticles with eco-friendly processes using Ganoderma lucidum extract and evaluation of their theranostic applications. *J. Nanomater.* Vol. 2021, pp. ID 6135920.

[8]. Pei JJ, Yan Y, Jayaraman S, Rajagopal P, Natarajan PM, et al. (2024). A review on advancements in the application of starch-based nanomaterials in biomedicine: Precision drug delivery and cancer therapy. *Int. J. Biol. Macromol.* Vol. 265(P1), pp. ID 130746.

[9]. Vasileva P, Donkova B, Karadjova I, Dushkin C. (2011). Synthesis of starch-stabilized silver nanoparticles and their application as a surface plasmon resonance-based sensor of hydrogen peroxide. *Colloids Surfaces A Physicochem. Eng. Asp.* Vol. 382(1–3), pp. 203–10.

[10]. Hebeish A, Shaheen TI, El-Naggar ME. (2016). Solid state synthesis of starch-capped silver nanoparticles. *Int. J. Biol. Macromol.* Vol. 87, pp. 70–76.

[11]. Bui TQ, Ngo HTM, Tran HT. (2018). Surface-protective assistance of ultrasound in synthesis of superparamagnetic magnetite nanoparticles and in preparation of mono-core magnetite-silica nanocomposites. *J. Sci. Adv. Mater. Devices*. Vol. 3(3), pp. 323–30.

[12]. Hangxun X, Zeiger BW, Suslick KS. (2013). Sonochemical synthesis of nanomaterials. *Chem. Soc. Rev.* Vol. 42(7), pp. 2555–67.

[13]. Scherrer P. (1912). Bestimmung der inneren Struktur und der Größe von Kolloidteilchen mittels Röntgenstrahlen. *Kolloidchem. Ein Lehrb.* Vol. 277(1916), pp. 387–409.

[14]. Amirjani A, Firouzi F, Haghshenas DF. (2020). Predicting the Size of Silver Nanoparticles from Their Optical Properties. *Plasmonics*. Vol. 15(4), pp. 1077–82.

[15]. Paramelle D, Sadovoy A, Gorelik S, Free P, Hobley J, Fernig DG. (2014). A rapid method to estimate the concentration of citrate capped silver nanoparticles from UV-visible light spectra. *Analyst*. Vol. 139(19), pp. 4855–61.

[16]. Abdullah AHD, Chalimah S, Primadona I, Hanantyo MHG. (2018). Physical and chemical properties of corn,cassava, and potato starchs. *IOP Conf. Ser. Earth Environ. Sci.* Vol. 160, pp. ID 012003.

TỔNG HỢP HÓA SIÊU ÂM VẬT LIỆU NANO BẠC TRÊN NỀN TINH BỘT VÀ THỬ NGHIỆM ĐÁNH GIÁ KHẢ NĂNG GẮN KẾT DOXORUBICIN

Trần Ngọc Diễm[1], Nguyễn Vĩnh Phú[2], Nguyễn Thị Thanh Tuyền[1], Ngô Khoa Quang[3], Bùi Quang Thành*[1]

[1]Khoa Hóa học, Trường Đại học Khoa học, Đại học Huế

[2]Khoa Cơ bản, Trường Đại học Y - Dược, Đại học Huế

[3]Khoa Điện, Điện tử và Công nghệ vật liệu, Trường Đại học Khoa học, Đại học Huế

*Email: thanh.bui@hueuni.edu.vn

TÓM TẮT

Vật liệu nano bạc (AgNPs) có ái lực với doxorubicin đáp ứng theo pH, nhưng còn hạn chế liên quan ổn định trong nước và độc tính từ quá trình tổng hợp. Nghiên cứu này khảo sát yếu tố ảnh hưởng tổng hợp xanh AgNPs, sau đó thử nghiệm sơ bộ khả năng gắn kết doxorubicin. Quy trình tối ưu chỉ sử dụng các chất tương thích sinh học, gồm: $AgNO_3$ (bạc), D-glucose (khử), starch (vệ), and NaOH (điều chỉnh pH), kết hợp siêu âm (42 kHz; 100 W) ở nhiệt độ phòng (25 °C). AgNPs trên nền tinh bột được tổng hợp thành công và phân tích đặc trưng bằng UV-Vis (λ_a 400 nm; I_a 3.0-3.5 abs., $\overline{D}_{\text{size(UV–Vis)}}$ 20-45 nm), XRD (2θ = 38.1° (111), 44.3° (200), 64.4° (220), 77.4° (311); JCPDS 04-0783; $\overline{D}_{\text{size(XRD)}}$ ~15 nm), SEM (hình thái: AgNPs nền tinh bột; $\overline{D}_{\text{size(SEM)}}$ 10-30 nm), EDX (C: 0.285 keV; O: 0.525 keV; Na: 1.044 keV; Ag: ~3 keV), và FT-IR (không thay đổi nhóm chức). Hệ vật liệu được chứng minh khả năng gắn kết và giải phóng doxorubicin đáp ứng pH bằng UV-Vis. Kết quả tạo tiền đề cho các nghiên cứu tiếp nối và thử nghiệm thực tế.

Từ khóa: doxorubicin, tổng hợp xanh, phản hồi pH, hóa siêu âm, nano bạc